Somayeh Hashemi-Uderji, Mohammad Abdollahi-Alibeik* and Reza Ranjbar-Karimi

FSM-16-SO_3H nanoparticles as a novel heterogeneous catalyst: preparation, characterization, and catalytic application in the synthesis of polyhydroquinolines

https://doi.org/10.1515/mgmc-2018-0006
Received February 1, 2018; accepted July 4, 2018

Abstract: FSM-16-SO_3H nanoparticles were prepared using a sol-gel method at room temperature. The prepared FSM-16-SO_3H was used to catalyze the synthesis of polyhydroquinolines through a one-pot, four-component reaction of aldehydes, dimedone, ethyl cyanoacetate, and ammonium acetate under reflux condition in EtOH as a green solvent. To investigate the textural properties of the prepared catalyst, various techniques were applied such as X-ray diffraction, Fourier transform infrared spectroscopy, scanning electron microscope, and Brunauer–Emmett–Teller. High catalytic activity, easy handling, and thermal stability are the superior properties that could be denoted after successive investigations of this catalyst. In addition, the catalyst can be recovered easily and reused effectively for several cycles.

Keywords: FSM-16-SO_3H; Hantzsch reaction; nanoparticle; polyhydroquinoline; sol-gel.

Introduction

Polyhydroquinoline and 1,4-dihydropyridine (1,4-DHP) derivatives have attracted noticeable concern because they have diverse biological activities such as geroprotective, vasodilator, antitumor, bronchodilator, hepatoprotective, antiatherosclerotic, calcium channel blocker, and antidiabetic activity (Davis and Davis, 1979; Bretzel et al., 1992, 1993; Boer and Gekeler, 1995; Klusa, 1995). Recently, research has shown that 1,4-DHPs exhibit diverse medicinal usage, which includes neuroprotectant and platelet antiaggregatory activity, in addition to cerebral anti-ischemic activity in the treatment of Alzheimer's disease and as a chemosensitizer in tumor therapy (Pastan and Gottesman, 1987). Moreover, these compounds can be used for their antioxidant protective effect in addition to their pharmacological activities (Mason et al., 1999). Thus, the synthesis of these heterocyclic compounds is of much importance.

1,4-DHPs are generally achieved using the classic Hantzsch method, which involves the condensation of an aldehyde with ethyl acetoacetate and ammonia in acetic acid or by refluxing in alcohol (Hantzsch, 1882). This method, however, involves long reaction times and the use of a large quantity of volatile organic solvents and generally gives low yields. Several catalysts such as ionic liquid (Khaligh, 2016), Baker's yeast (Kumar and Maurya, 2007), silica gel/$NaHSO_4$ (Adharvana Chari and Syamasundar, 2005), $Yb(OTf)_3$ (Wang et al., 2005), $Sc(OTf)_3$ (Donelson et al., 2006), ZnO (Moghaddam et al., 2009), MgO (Ranjbar-Karimi et al., 2011), ceric ammonium nitrate (Ko and Yao, 2006), polymers (Dondoni et al., 2004), $HClO_4$-SiO_2 (Maheswara et al., 2006), HY-zeolites (Das et al., 2006), montmorillonite K-10 (Song et al., 2005), *p*-TSA (Kumar and Maurya, 2008), L-proline (Karade et al., 2007), $ZrCl_4$ (Reddy and Raghu, 2008), MCM-41 (Nagarapu et al., 2007), $Hf(NPf_2)_4$ (Hong et al., 2010), $Cu(OTf)_2$ (Pasunooti et al., 2010), Fe_3O_4@B-MCM-41 (Abdollahi-Alibeik and Rezaeipoor-Anari, 2016), and MCM-41-OBF_2 (Abdollahi-Alibeik and Rezaeipoor-Anari, 2015) have been used to improve Hantzsch reaction conditions. Also, several energy sources such as microwaves (Tu et al., 2006), grinding techniques (Kumar et al., 2008), ultrasound (Guo and Yuan, 2010), and solar heat (Mekheimer et al., 2008) have been reported for this purpose. Furthermore, the development of an efficient and versatile method for the preparation of 1,4-DHPs and polyhydroquinoline is an active ongoing research area and there is scope for further improvement toward milder reaction conditions and to access higher yields.

Recently, heterogeneous catalysts have become attractive from both economic and industrial points of view as compared with homogeneous catalysts. In general, nanoscale heterogeneous catalysts offer higher surface area and lower coordinating sites, which are responsible for the higher catalytic activity.

Mesoporous silica as a nanostructured material with highly ordered pores and high surface area, such as FSM-16 and MCM-41, have attracted considerable interest in the fields of adsorption science and catalysis chemistry

***Corresponding author: Mohammad Abdollahi-Alibeik,** Department of Chemistry, Yazd University, Yazd 89158-13149, Iran, Tel.: +98-35-31232659, Fax: +98-35-38210644, e-mail: abdollahi@yazd.ac.ir, moabdollahi@gmail.com
Somayeh Hashemi-Uderji: Department of Chemistry, Yazd University, Yazd 89158-13149, Iran
Reza Ranjbar-Karimi: Department of Chemistry, Faculty of Science, Vali-e-Asr University, Rafsanjan 77176, Iran

(Yanagisawa et al., 1990; Inagaki et al., 1993; Inagaki et al., 1996; Abdollahi-Alibeik and Pouriayevali, 2011; Abdollahi-Alibeik and Rezaeipoor-Anari, 2014). Mesoporous silica of the FSM type, which is composed of siliceous sheets, was synthesized by Inagaki and co-workers (Inagaki et al., 1993). Folded sheet silicate mesoporous material (FSM-16) was first synthesized by ion exchange of interlayer Na ions of the layered polysilicate kanemite ($NaHSi_2O_5 \cdot 3H_2O$) with surfactant (Yanagisawa et al., 1990; Inagaki et al., 1993).

Considering the fact that FSM-16 offers high surface area, many functional groups can be anchored on the inner surface of the mesopores to enhance the catalytic activity and the acidic or basic characteristics of organic transformations.

In this research, we report the preparation and characterization of FSM-16-SO_3H as a novel heterogeneous acid catalyst by functionalization of silanol groups on the surface of FSM-16 with -SO_3H groups (Scheme 1).

The catalytic activity of FSM-16-SO_3H was also studied in the reaction of various types of aldehydes, dimedone, ethyl cyanoacetate, and ammonium acetate for the synthesis of polyhydroquinolines (Scheme 2).

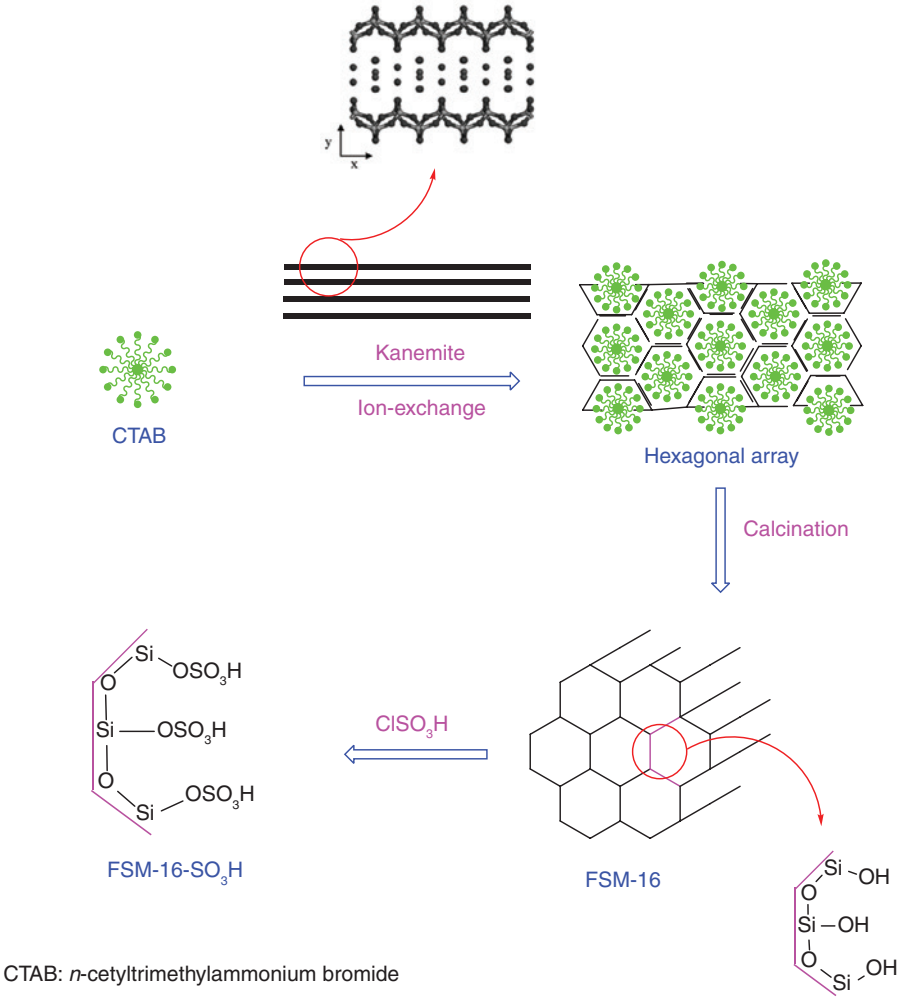

CTAB: *n*-cetyltrimethylammonium bromide

Scheme 1: Schematic representation for the preparation of FSM-16-SO_3H.

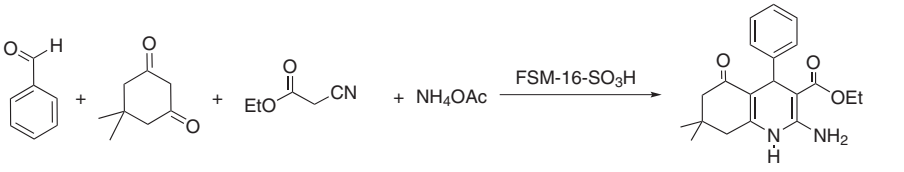

Scheme 2: Synthesis of polyhydroquinolines using a one-pot, four-component reaction in the presence of FSM-16-SO_3H.

Results and discussion

The catalyst characterization

FSM-16 and FSM-16-SO_3H were characterized using Fourier transform infrared spectroscopy (FT-IR), scanning electron microscope (SEM), Brunauer–Emmett–Teller (BET), and X-ray diffraction (XRD) techniques. The SEM micrographs of FSM-16 and FSM-16-SO_3H are shown in Figure 1A and B, respectively. SEM micrographs show spherical nanoparticles with sizes of approximately 100 nm. Both materials have similar texture and there is no significant difference.

The FT-IR spectra of FSM-16 and FSM-16-SO_3H are shown in Figure 2. The spectrum of FSM-16 (Figure 2A) shows characteristic peaks at 1216, 1082, and 804 cm^{-1} due to symmetric and asymmetric stretching vibrations of Si-O-Si and also the peak of 966 cm^{-1} due to Si-OH groups. The peak at 463 cm^{-1} is assigned to the bending vibration of Si-O-Si. For FSM-16-SO_3H (Figure 2B), the FT-IR bands of the O=S=O asymmetric and symmetric stretching modes lie in 1120–1230 and 1010–1080 cm^{-1}, respectively, and that of the S-O stretching mode lies in 600 cm^{-1}. The FT-IR spectrum of FSM-16-SO_3H shows the overlap of asymmetric and symmetric stretching bands of SO_2 with Si-O-Si stretching bands in the region of 1000–1250 cm^{-1}, which results in an increase of intensity of this peak.

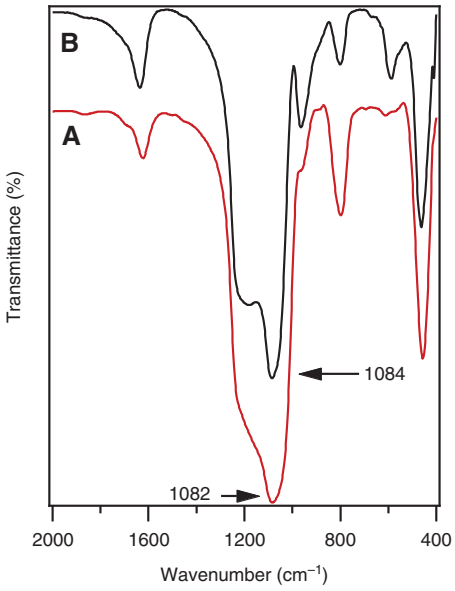

Figure 2: FT-IR spectra of (A) FSM-16 and (B) FSM-16-SO_3H.

The low angle XRD patterns of FSM-16 and FSM-16-SO_3H are shown in Figure 3. The characteristic peaks

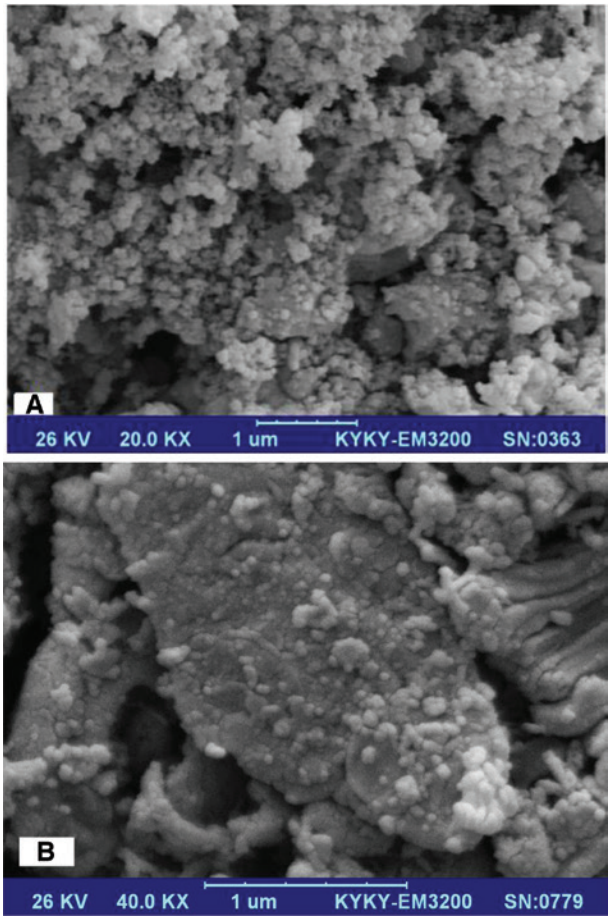

Figure 1: SEM images of (A) FSM-16 and (B) FSM-16-SO_3H.

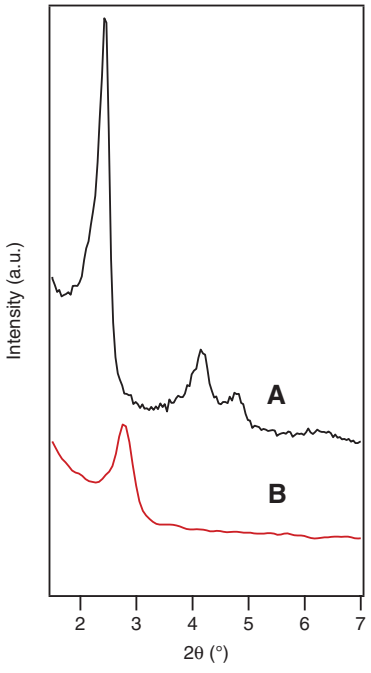

Figure 3: Low angle XRD patterns of (A) FSM-16 and (B) FSM-16-SO_3H.

of FSM-16 (Figure 3A) appeared at $2\theta = 2.38°$, 4.11°, and 4.73° in accordance with the literature (Araki et al., 2003). As shown in Figure 3B, after surface modification with SO_3H groups, the intensity of the main peak ($2\theta = 2.38°$) decreased and shifted to the higher angle ($2\theta = 2.76°$). Any increase in the width of the main peak of the FSM-16-SO_3H is due to a decrease in the long-range order of the hexagonal mesostructure of FSM-16 after the incorporation of -SO_3H groups into the channels of FSM-16. The shift in the main peak of FSM-16-SO_3H to a higher angle is due to a decrease in the pore diameter because of the insertion of sulfonic acid groups on the inner surface of mesopores.

The distribution of both Brønsted and Lewis acid sites of FSM-16-SO_3H was detected using FT-IR spectroscopy by means of pyridine absorption. Figure 4 shows the pyridine adsorbed spectra of FSM-16-SO_3H heated at various temperatures. The spectrum of pyridine adsorbed FSM-16 shows only peaks of pyridine-bonded Lewis acid sites at 1446 and 1598 cm^{-1} (Figure 4B). The spectrum of pyridine-adsorbed FSM-16-SO_3H before heat treatment (Figure 4C) shows the contribution of the pyridine adducts in the region of 1400–1650 cm^{-1}. The peak at 1487 cm^{-1} is attributed to the combination of pyridine bonded to Lewis and Brønsted acid sites. The peak appearing at 1530 cm^{-1} is assigned to Brønsted acid sites (pyridinum ion). The peak at 1603 cm^{-1} is attributed to the pyridine-bonded Lewis acid sites of the catalyst. The peak at 1633 cm^{-1} in the spectrum of the catalyst before treatment with pyridine (Figure 4A) is due to the presence of water during the preparation of the pellet sample. This sharp peak overlapped with another weak peak from the Brønsted acid site at 1642 cm^{-1}. However, these results confirm the distribution of both Brønsted and Lewis acid sites on the surface of the catalyst. As shown in Figure 4B–E, with increasing temperature, the characteristic peak of Lewis acid sites at 1603 cm^{-1} and the peak of Brønsted acid sites at 1530 cm^{-1} still remained. These results confirm that -SO_3H functionalization has strengthened both Brønsted and Lewis acid sites on the catalyst.

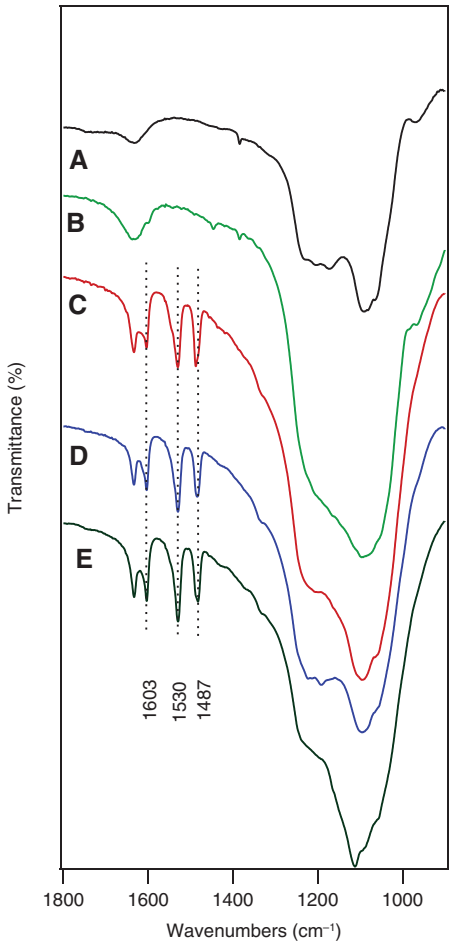

Figure 4: FT-IR spectra of (A) FSM-16-SO_3H, (B) pyridine adsorbed FSM-16, and (C) FSM-16-SO_3H at ambient temperature; pyridine-adsorbed FSM-16-SO_3H heated at (D) 100°C and (E) 200°C.

The strength and number of acid sites of the catalysts were determined by potentiometric titration of samples with 0.02 N solution of *n*-butylamine in acetonitrile. According to this method, the initial electrode potential (E_i) indicates the strength of the acid sites, and the meq of the consumed base indicates the number of acid sites (Pizzio et al., 2003). As shown in Figure 5, the very low initial potential of FSM-16 shows that the acid strength of these samples is very low. By placing the -SO_3H groups on the surface of FSM-16, FSM-16-SO_3H displays higher strength than that of FSM-16. Because of the higher meq of the used base per gram of the FSM-16-SO_3H, this sample also has a higher number of acidic sites than FSM-16.

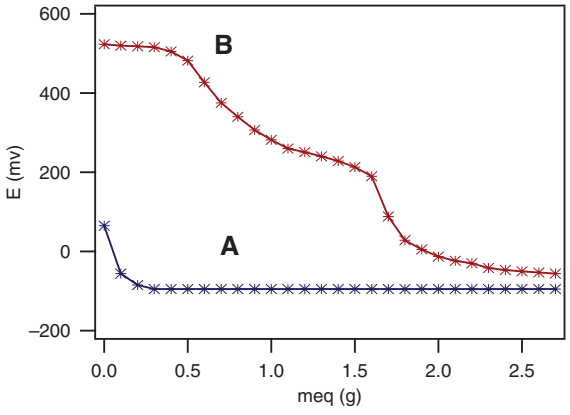

Figure 5: Potentiometric titration of (A) FSM-16 and (B) FSM-16-SO_3H.

To investigate the number of -SO_3H acidic sites supported on the FSM-16, the elemental composition of the FSM-16-SO_3H was determined using energy dispersive X-ray (EDX) analysis, and the results are shown in Figure 6 and Table 1. Based on these results, the amount of sulfur in the FSM-16-SO_3H was 7.08 wt.%, and thus the number of -SO_3H on the catalyst was 0.87 mmol per gram of FSM-16-SO_3H.

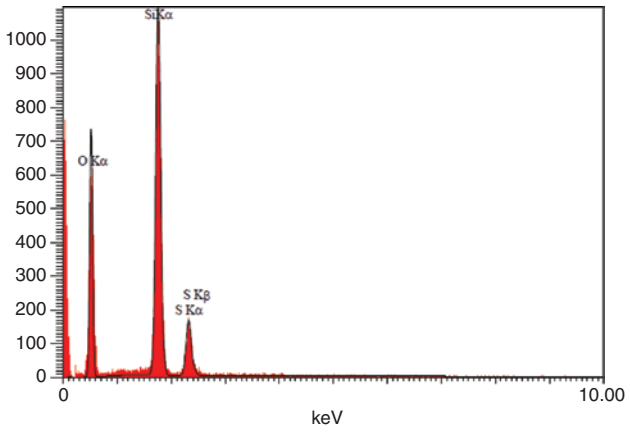

Figure 6: Energy-dispersive X-ray spectrum of FSM-16-SO_3H.

Table 1: Elemental composition of FSM-16-SO_3H.

Element	O	Si	S
wt.%	61.31	31.60	7.08

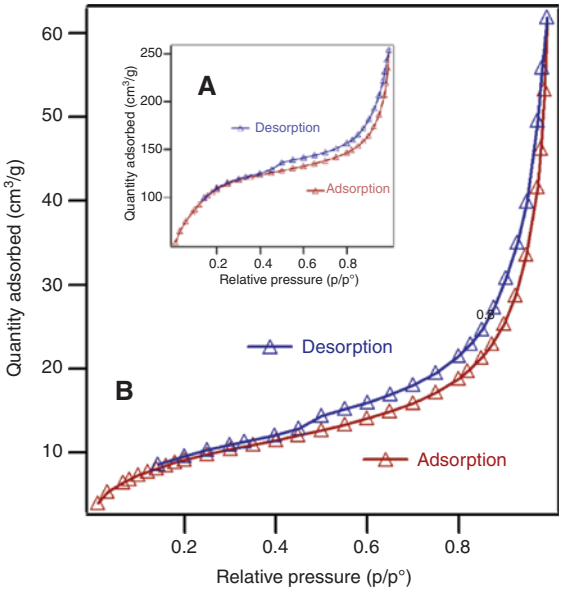

Figure 7: N_2 adsorption–desorption isotherms of (A) FSM-16 and (B) FSM-16-SO_3H.

Figure 7 shows the N_2 adsorption–desorption isotherms of the FSM-16 and FSM-16-SO_3H catalysts. In the isotherms of FSM-16, a mesoporous inflection was observed at the medium p/p° partial pressure region (p/p° = 0.1–0.3) due to the capillary condensation of N_2 in the mesopores. A sharper hysteresis was observed at higher p/p° (p/p° > 0.8) for both catalysts. The hysteresis in this region is because of the condensation of N_2 within the voids formed by nanoparticles. In the isotherms of FSM-16-SO_3H, the curvature of the mesoporous structure in the area of P/P° = 0.2–0.4 decreased because the hexagonal cavities were occupied by -SO_3H groups. The textural properties of FSM-16-SO_3H were also studied by N_2 adsorption–desorption isotherms. According to the obtained results, the BET surface area for FSM-16-SO_3H was measured to be 634 m^2/g and the average pore diameter using the Barret–Joyner–Halenda desorption method was calculated to be 5.97 nm.

Catalytic activity of FSM-16-SO_3H

After the catalyst characterization was done successfully, the catalytic activity of FSM-16-SO_3H nanoparticles was investigated in the synthesis of polyhydroquinolines. Initially, the reaction of benzaldehyde, dimedone, ethyl cyanoacetate, and ammonium acetate was selected as the model reaction and the results are summarized in Table 2.

The effect of solvent and temperature was investigated by performing the model reaction in the presence of 40 mg of catalyst in various solvents and temperatures (Table 2, entries 1–6). Among them, ethanol was found to be the best solvent at reflux condition in terms of the reaction time and yield of product (Table 2, entry 6). The lower yield and longer reaction time was achieved by performing the model reaction in the presence of ethanol as the solvent at r.t. condition (Table 2, entry 5).

To optimize the required catalyst amount, the model reaction was also performed in the presence of various amounts of catalyst, and according to the obtained results (Table 2, entries 6 and 9–11), 40 mg of the catalyst was chosen as the best amount. Clearly, the FSM-16 support strongly affected the efficiency of the heterogeneous catalyst. To show this, the model reaction in the presence of 40 mg FSM-16 was performed under the same reaction conditions and lower yield of the product was obtained after 90 min (Table 2, entry 8).

The scope and generality of this methodology has been illustrated with respect to the reaction of different types of benzaldehydes that have electron-withdrawing and electron-donating groups with dimedone, ammonium

Table 2: Optimization of the reaction conditions for the synthesis of polyhydroquinoline in the presence of FSM-16-SO_3H.[a]

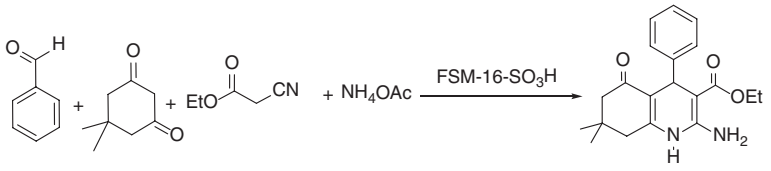

Entry	Catalyst	Catalyst amount (mg)	Solvent	Time (min)	Yield (%)[b]
1	FSM-16-SO_3H	40	$CHCl_3$	180	76
2	FSM-16-SO_3H	40	CH_2Cl_2	240	71
3	FSM-16-SO_3H	40	MeOH	30	88
4	FSM-16-SO_3H	40	CH_3CN	60	82
5	FSM-16-SO_3H	40	EtOH[c]	240	81
6[d]	**FSM-16-SO_3H**	**40**	**EtOH**	**30**	**93**
7	–	0	EtOH	240	30
8	FSM-16	40	EtOH	90	79
9	FSM-16-SO_3H	20	EtOH	35	87
10	FSM-16-SO_3H	30	EtOH	30	84
11	FSM-16-SO_3H	50	EtOH	45	88

[a]Reaction condition: benzaldehyde (1 mmol), dimedone (1 mmol), ethyl cyanoacetate (1.1 mmol), and ammonium acetate (1.2 mmol) at reflux condition.
[b]Isolated yield.
[c]Reaction was carried out at room temperature.
[d]Bolded row represent optimized condition.

acetate, and ethyl cyanoacetate and the results are summarized in Table 3.

The reaction of various types of aryl aldehydes with both electron-donating and electron-withdrawing substituents were carried out under optimal conditions and the corresponding polyhydroquinolines were obtained in high to excellent yields (Table 3, entries 2–11). As exemplified in Table 3, this protocol is rather general for a wide variety of electron-rich as well as electron-deficient aromatic aldehydes. Although a regular trend was not observed based on the activity of aldehyde derivatives, the results in Table 3 show that aldehydes with electron-withdrawing groups such as -NO_2, Cl, Br, and -F have maximum rates of reaction.

To investigate the reusability of FSM-16-SO_3H, it was separated from the reaction mixture and washed with ethanol. The catalyst was dried in an oven at 120°C for 2 h. The recycled catalyst was reused in the model reaction. The catalyst was found to be reusable for at least three cycles without considerable loss of activity (Table 4).

Table 5 shows a comparison between the activity of the FSM-16-SO_3H and the other reported catalysts for the polyhydroquinoline synthesis through reaction of benzaldehyde, dimedone, ethyl cyanoacetate, and ammonium acetate. Results show that FSM-16-SO_3H is comparable with other catalytic systems in terms of reaction time and/or yield.

Conclusion

In summary, we have developed a novel, mild, and efficient strategy for the synthesis of polyhydroquinoline from dimedone, aryl aldehydes, ammonium acetate, and ethyl cyanoacetate through Knoevenagel condensation followed by Michael addition reaction in the presence of FSM-16-SO_3H as a heterogeneous solid acid catalyst. The catalyst was texturally investigated using various techniques such as SEM, XRD, FT-IR, and BET, and the results show that the mesoporous structure of the bare support (FSM-16) was maintained during sulfonic acid functionalization. In addition, the characteristic acidity of the obtained catalyst was proved by pyridine adsorption and potentiometric titration techniques. After successful characterization of the catalyst, catalytic activity was investigated in the synthesis of polyhydroquinolines and optimal reaction conditions were obtained. The generality of the catalytic process was confirmed using various precursors and the corresponding products were obtained in good to excellent yields and characterized by NMR and FT-IR. A reusability test shows that the mesoporous FSM-16-SO_3H catalyst is reusable with moderate decrease in activity. High yields of the products, very simple workup, and ease of the catalyst recovery are some of the advantages of using this catalyst.

Table 3: Synthesis of polyhydroquinolines in the presence of FSM-16-SO_3H.

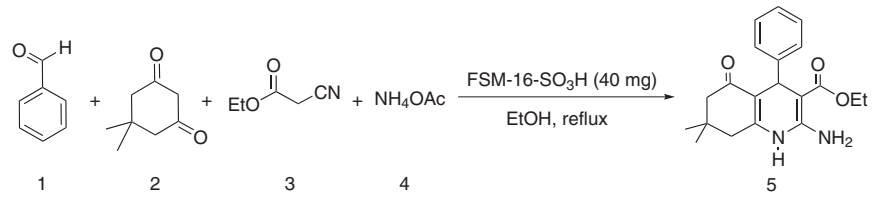

Entry	Aldehyde (1)	Polyhydroquinoline (5)	Time (min)	Yield[a] (%)	mp (°C)	
					Found	Lit. [ref]
a	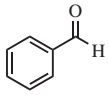	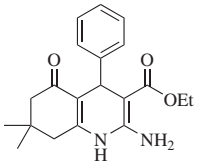	30	93	157–160	150–155 (Kumar et al., 2008)
b	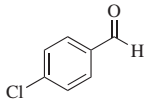	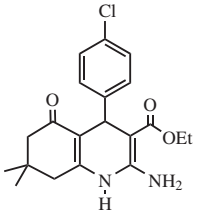	20	88	155–157	150–153 (Abdollahi-Alibeik and Rezaeipoor-Anari, 2016)
c	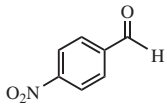	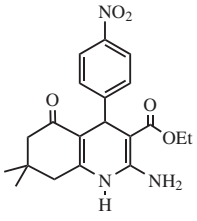	20	94	190–195	190–195 (Abdollahi-Alibeik and Rezaeipoor-Anari, 2016)
d	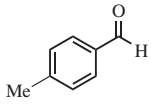	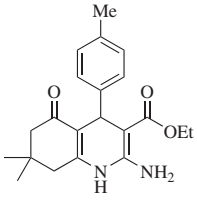	40	90	139–141	135–137 (Kumar et al., 2008)
e	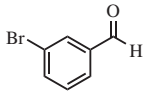	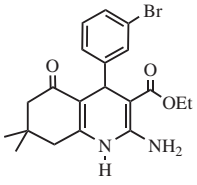	15	88	135–136	140–143 (Abdollahi-Alibeik and Rezaeipoor-Anari, 2016)
f	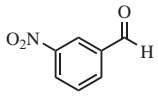	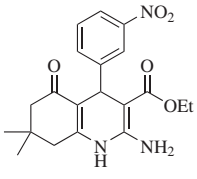	10	89	183–184	–
g	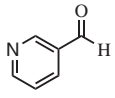	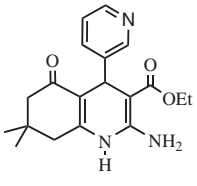	60	80	172–175	179–181 (Abdollahi-Alibeik and Rezaeipoor-Anari, 2016)

Table 3 (continued)

Entry	Aldehyde (1)	Polyhydroquinoline (5)	Time (min)	Yield[a] (%)	mp (°C)	
					Found	Lit. [ref]
h	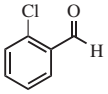	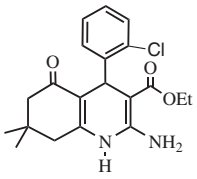	5	94	182–183	183–185 (Abdollahi-Alibeik and Rezaeipoor-Anari, 2016)
i	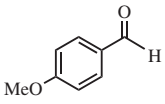	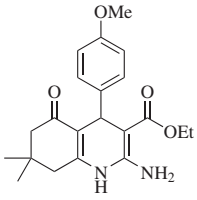	55	83	128–130	122–125 (Kumar et al., 2008)
j	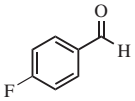	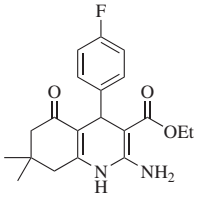	25	93	155–158	–
k	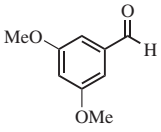	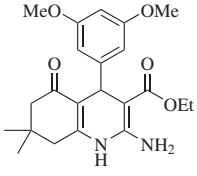	15	91	222–226	–

[a]Isolated yield.

Table 4: Recycling of FSM-16-SO_3H nanoparticles.

Run	Yield (%)[a]	Time
1	93	30
2	90	40
3	87	45

[a]Isolated yields.

Experimental

Materials and methods

All chemicals were commercial grade and were used as-received. The reactions were monitored using thin layer chromatography (TLC). The yields of products refer to isolated compounds. Melting points

Table 5: The comparative study of the activity of FSM-16-SO_3H with other catalysts.

Entry	Catalyst	Solvent	Temperature (°C)	Time (min)	Yield[a]	Ref.
1	FSM-16-SO_3H	Ethanol	Reflux	30	93	This work
2	$PdCl_2$	THF	Reflux	240	87	(Saha and Pal, 2011)
3	ZnO NPs	Solvent free	r.t.	30	88	(Kassaee et al., 2010)
4	MCM-41-OBF_2	Ethanol	Reflux	50	91.5	(Abdollahi-Alibeik and Rezaeipoor-Anari, 2015)
5	Fe_3O_4@B-MCM-41	Ethanol	Reflux	40	90	(Abdollahi-Alibeik and Rezaeipoor-Anari, 2016)
6	ClO^{4-}/Zr-MCM-41	Ethanol	Reflux	40	94	(Abdollahi-Alibeik and Hoseinikhah, 2016)
7	(Grinding)	Solvent free	r.t.	20	72	(Kumar et al., 2008)
8	(Microwave irradiation)	Ethanol	50	5	91	(Saha et al., 2013)

were obtained with a Buchi B-540 apparatus and are uncorrected. ^{1}H NMR and ^{13}C NMR spectra of polyhydroquinolines were recorded in DMSO-d_6 on a Bruker DRX-500 AVANCE spectrometer (500 MHz for ^{1}H and 125.72 MHz for ^{13}C). Infrared spectra of the reaction products and catalysts were recorded on a Bruker FT-IR Equinax-55 in KBr disks. The XRD patterns were recorded on a Bruker D8 ADVANCE X-ray diffractometer using Ni-filtered CuKa radiation. The morphology was studied using a KYKY-EM3200 SEM. The BET surface area was measured using a micromeritics model ASAP2020 from the nitrogen adsorption–desorption isotherms at 77 K. All samples were degassed at 120°C under flowing nitrogen for 2 h. The specific surface area (S_{BET}) was calculated from the adsorption data using the BET equation, and the pore volume (V_{pore}) was estimated from the volume of adsorbed N_2 at relative pressure (p/p°) of 0.99. The pore size distribution was calculated using the Barret–Joyner–Halenda method.

Preparation of FSM-16 nanoparticles

A typical procedure for the preparation of kanemite was as follows: to a solution of NaOH (3 g) dissolved in deionized water (30 mL), tetraethylortosilicate (16.6 mL) was added dropwise and then the mixture was stirred for another 12 h at room temperature. The solution was transferred into an oven and heated at 355 K for 4 h. The resultant product was calcined at 923 K for 5 h to obtain δ-$Na_2Si_2O_5$ (kanemite). The kanemite was deliquescent and immediately used for further treatment. Kanemite (5 g) was dispersed in deionized water (50 mL) and then stirred for 3 h at 300 K. Then, the suspension was filtered out to obtain wet kanemite paste. All of the kanemite paste was dispersed in an aqueous solution (40 mL) of cetyltrimethylammonium bromide (0.125 mol L^{-1}) and then stirred at 343 K for 3 h. The pH value of the suspension was 11.5–12.5 at this stage. Afterward, the pH value was adjusted carefully to 8.5 by adding 2 mol L^{-1} of hydrochloric acid with stirring. The suspension was continuously stirred at 343 K for 3 h while keeping the pH value at 8–9. After cooling to r.t., the solids were separated using a centrifuge and washed with distilled water (20 mL) and dried in an oven at 393 K for 2 h to yield mesoporous silicate, FSM-16, while retaining the template. The product was calcined at 823 K to burn off the surfactant to obtain the final FSM-16.

Preparation of FSM-16-SO_3H nanoparticles

FSM-16 (0.278 g) was added to dry CH_2Cl_2 (3 mL) in a 5 mL round-bottomed flask equipped with a gas outlet tube and a dropping funnel containing a solution of chlorosulfonic acid (0.6 mL) in dry CH_2Cl_2 (4.5 mL). The chlorosulfonic acid solution was added dropwise to the obtained suspension over a period of 30 min at room temperature. After completion of the reaction, the sediment was separated using a centrifuge and then washed with deionized water (2×3 mL). The obtained solid was dried in an oven at 120°C for 2 h to obtain FSM-16-SO_3H.

General procedure for the synthesis of polyhydroquinoline derivatives in the presence of FSM-16-SO_3H

A mixture of dimedone (1 mmol), aldehyde (1 mmol), ethyl cyanoacetate (1.1 mmol), ammonium acetate (1.2 mmol), and a catalytic amount of FSM-16-SO_3H (40 mg) was stirred in ethanol (1.5 mL) under reflux conditions. After completion of the reaction (monitored by TLC, eluent; *n*-hexane: ethyl acetate, 1:1), the catalyst was separated from the reaction mixture using a centrifuge and washed with ethanol (2×3 mL). After evaporation of solvent, the crude products were crystallized from ethanol to give pure polyhydroquinolines.

Physical and spectroscopic data for selected compounds

Ethyl 2-amino-1,4,5,6,7,8-hexahydro-7,7-dimethyl-5-oxo-4-phenylquinoline-3-carboxylate (5a): Light yellow solid, mp 157°C–160°C [150°C–155°C Lit. (Kumar et al., 2008)]. IR (KBr) υ_{max} (cm^{-1}): 3402 (NH_2), 3289 (NH_2), 3204 (NH), 1692 (C=O), 1659 (C=O), 1610 (C=C), 1291 (C-O), 1029 (C-N). ^{1}H NMR (500 MHz, $CDCl_3$): δ (ppm) = 1.01 (s, 3H), 1.14 (s, 3H), 1.21 (t, 3H, J = 5.3 Hz), 2.19 (d, 1H, J = 16.5 Hz), 2.26 (d, 1H, J = 16.5 Hz), 2.47 (s, 2H), 4.02–4.12 (m, 2H), 4.74 (s, 1H), 6.22 (s, 2H, NH_2), 7.14 (t, 1H, J = 6.6 Hz), 7.24 (t, 2H, J = 7.2 Hz), 7.30 (d, 2H, J = 6.7 Hz). ^{13}C NMR (125.72 MHz, $CDCl_3$): δ (ppm) = 14.6, 27.8, 29.5, 32.7, 34.3, 41.1, 51.2, 60.1, 81.2, 117.3, 126.4, 128.2, 128.6, 146.2, 158.8, 161.8, 169.5, 196.9.

Ethyl 2-amino-4-(4-chlorophenyl)-1,4,5,6,7,8-hexahydro-7,7-dimethyl-5-oxoquinoline-3-carboxylate (5b): Light yellow solid, mp 155°C–157°C [150°C–153°C Lit. (Abdollahi-Alibeik and Rezaeipoor-Anari, 2016)]. IR (KBr) υ_{max} (cm^{-1}): 3479 (NH_2), 3327 (NH_2), 3204 (NH), 1689 (C=O), 1659 (C=O), 1620 (C=C), 1295 (C-O), 1038 (C-N). ^{1}H NMR (500 MHz, $CDCl_3$): δ (ppm) = 1.00 (s, 3H), 1.14 (s, 3H), 1.18 (t, 3H, J = 8.8 Hz), 2.19 (d, 1H, J = 16.5 Hz), 2.27 (d, 1H, J = 16.5 Hz), 2.46 (s, 2H), 4.02–4.12 (m, 2H), 4.71 (s, 1H), 6.22 (s, 2H, NH_2), 7.21 (d, 2H, J = 4.0 Hz), 7.24 (d, 2H, J = 4.0 Hz). ^{13}C NMR (125.72 MHz, $CDCl_3$): δ (ppm) = 14.6, 27.8, 29.5, 32.7, 33.8, 41.1, 51.1, 60.2, 80.8, 116.8, 128.3, 130.1, 144.8, 158.7, 161.9, 169.3, 196.7.

Ethyl 2-amino-1,4,5,6,7,8-hexahydro-7,7-dimethyl-4-(4-nitrophenyl)-5-oxoquinoline-3-carboxylate (5c): Light yellow solid, mp 190°C–195°C [190°C–195°C Lit. (Abdollahi-Alibeik and Rezaeipoor-Anari, 2016)]. IR (KBr) υ_{max} (cm^{-1}): 3474 (NH_2), 3337 (NH_2), 3201 (NH), 1689 (C=O), 1658 (C=O), 1621 (C=C), 1296 (C-O), 1039 (C-N). ^{1}H NMR (500 MHz, $CDCl_3$): δ (ppm) = 0.99 (s, 3H), 1.15 (s, 3H), 1.66 (t, 3H, J = 7.1 Hz), 2.17 (d, 1H, J = 16.5 Hz), 2.27 (d, 1H, J = 16.5 Hz), 2.49 (s, 2H), 3.99–4.10 (m, 2H), 4.83 (s, 1H), 6.31 (s, 2H, NH_2), 7.47 (d, 2H, J = 8.7 Hz), 8.12 (d, 2H, J = 8.7 Hz). ^{13}C NMR (125.72 MHz, $CDCl_3$): δ (ppm) = 14.6, 27.7, 29.5, 32.7, 34.7, 41.1, 51.0, 60.3, 79.8, 116.0, 123.6, 129.6, 153.9, 158.8, 162.4, 169.0, 196.6.

Ethyl 2-amino-1,4,5,6,7,8-hexahydro-7,7-dimethyl-5-oxo-4-*p*-tolylquinoline-3-carboxylate (5d): Light yellow solid, mp 139°C–141°C [135°C–137°C Lit. (Kumar et al., 2008)]. IR (KBr) υ_{max} (cm^{-1}): 3407 (NH_2), 3293 (NH_2), 3222 (NH), 1691 (C=O), 1656 (C=O), 1622 (C=C), 1288 (C-O), 1034 (C-N). ^{1}H NMR (500 MHz, $CDCl_3$): δ (ppm) = 1.20 (s, 3H), 1.13 (s, 3H), 1.22 (t, 3H, J = 7.1 Hz), 2.19 (d, 1H, J = 16.0 Hz), 2.26 (d, 1H, J = 16.0 Hz), 2.33 (s, 3H), 2.46 (s, 2H), 4.04–4.12 (m, 2H), 4.71 (s, 1H), 6.22 (s, 2H, NH_2), 7.05 (d, 2H, J = 7.8 Hz), 7.18 (d, 2H, J = 8.0 Hz). ^{13}C NMR (125.72 MHz, $CDCl_3$): δ (ppm) = 14.7, 21.5, 27.9, 29.5, 32.7, 33.8, 41.1, 51.2, 60.1, 81.4, 117.4, 128.5, 128.9, 135.8, 143.3, 158.8, 161.7, 169.6, 196.8.

Ethyl 2-amino-4-(3-bromophenyl)-1,4,5,6,7,8-hexahydro-7,7-dimethyl-5-oxoquinoline-3-carboxylate (5e): Light yellow solid, mp 135°C–136°C [140°C–143°C Lit. (Abdollahi-Alibeik and Rezaeipoor-Anari, 2016)]. IR (KBr) υ_{max} (cm^{-1}): 3409 (NH_2), 3296 (NH_2), 3227 (NH),

1692 (C=O), 1657 (C=O), 1620 (C=C), 1288 (C-O), 1035 (C-N). ^{1}H NMR (500 MHz, $CDCl_3$): δ (ppm) = 1.02 (s, 3H), 1.13 (s, 3H), 1.20 (t, 3H, J = 7.0 Hz), 2.20 (d, 1H, J = 16.0 Hz), 2.26 (d, 1H, J = 16.0 Hz), 2.46 (s, 2H), 4.06–4.09 (m, 2H), 4.70 (s, 1H), 6.28 (s, 2H, NH_2), 7.10 (t, 1H, J = 7.6 Hz), 7.23 (d, 1H, J = 7.7 Hz), 7.26 (d, 1H, J = 7.8 Hz), 7.42 (s, 1H). ^{13}C NMR (125.72 MHz, $CDCl_3$): δ (ppm) = 14.6, 27.9, 29.5, 32.7, 34.2, 41.1, 51.1, 60.2, 80.5, 116.5, 122.3, 127.5, 129.6, 129.7, 131.8, 148.6, 158.7, 162.1, 169.3, 196.7.

Ethyl 2-amino-1,4,5,6,7,8-hexahydro-7,7-dimethyl-4-(3-nitrophenyl)-5-oxoquinoline-3-carboxylate (5f): Light yellow solid, mp 183°C–184°C. IR (KBr) υ_{max} (cm^{-1}): 3440 (NH_2), 3300 (NH_2), 3208 (NH), 1692 (C=O), 1671 (C=O), 1622 (C=C), 1251 (C-O), 1038 (C-N). ^{1}H NMR (500 MHz, $CDCl_3$): δ (ppm) = 1.00 (s, 3H), 1.13 (s, 3H), 1.17 (t, 3H, J = 7.1 Hz), 2.17 (d, 1H, J = 16.0 Hz), 2.27 (d, 1H, J = 16.0 Hz), 2.50 (s, 2H), 4.03–4.07 (m, 2H), 4.81 (s, 1H), 6.40 (s, 2H, NH_2), 7.40 (t, 1H, J = 7.9 Hz), 7.67 (d, 1H, J = 7.9 Hz), 8.00 (d, 1H, J = 7.9 Hz), 8.13 (s, 1H). ^{13}C NMR (125.72 MHz, $CDCl_3$): δ = 14.6, 27.7, 29.4, 32.6, 34.6, 41.0, 51.0, 60.3, 79.9, 116.0, 121.7, 123.6, 128.9, 135.3, 148.5, 148.6, 158.8, 162.5, 169.0, 196.7.

Ethyl 2-amino-7,7-dimethyl-5-oxo-4-(pyridin-3-yl)-1,4,5,6,7,8-hexahydroquinoline-3-carboxylate (5g): Light yellow solid, mp 172°C–175°C [179°C–181°C Lit. (Abdollahi-Alibeik and Rezaeipoor-Anari, 2016)]. IR (KBr) υ_{max} (cm^{-1}): 3440 (NH_2), 3335 (NH_2), 3200 (NH), 1690 (C=O), 1663 (C=O), 1622 (C=C), 1279 (C-O), 1040 (C-N). ^{1}H NMR (400MHz, ($CDCl_3$): δ (ppm) = 0.99 (s, 3H), 1.12 (s, 3H), 1.16 (t, 3H, J = 7.0 Hz), 2.17 (d, 1H, J = 16.2 Hz), 2.25 (d, 1H, J = 16.2 Hz), 2.46 (s, 2H), 4.03–4.04 (m, 2H), 4.71 (s, 1H), 6.29 (s, 2H, NH_2), 7.14–7.17 (m, 1H), 7.58–7.61 (m, 1H), 8.36–8.37 (m, 1H), 8.53 (s, 1H). ^{13}C NMR (100 MHz, ($CDCl_3$): δ (ppm) = 14, 27, 29, 31, 40, 50, 51, 60, 79, 116, 123, 136, 141, 147, 150, 159, 162, 169, 196. Anal. Calcd. for $C_{19}H_{23}N_3O_3$: C, 66.84; H, 6.79; N, 12.31. Found: C, 66.73; H, 6.61; N, 12.37.

Ethyl-2-amino-4-(2-chlorophenyl)-7,7-dimethyl-5-oxo-1,4,5,6,7,8-hexahydroquinoline-3-carboxylate (5h): White solid, mp 182°C–183°C [183°C–185°C Lit. (Abdollahi-Alibeik and Rezaeipoor-Anari, 2016)]. IR (KBr) υ_{max} (cm^{-1}): 3420 (NH_2), 3309 (NH_2), 3215 (NH), 1693 (C=O), 1655 (C=O), 1613 (C=C), 1294 (C-O), 1038 (C-N). ^{1}H NMR (400 MHz, DMSO-*d6*): δ (ppm) = 0.93 (s, 3H), 1.02 (t, 3H, J = 7.2 Hz), 1.03 (s, 3H), 2.02 (d, 1H, J = 16.1 Hz), 2.25 (d, 1H, J = 16.1 Hz), 2.39–2.59 (m, 2H), 3.91 (q, 2H, J = 7.0 Hz), 4.83 (s, 1H), 7.21–7.25 (m, 4H), 7.65 (s, 2H, NH_2). ^{13}C NMR (100 MHz, DMSO-*d6*): δ (ppm) = 14.1, 26.4, 28.6, 31.7, 32.2, 49.9, 55.7, 76.3, 113.9, 126.3, 127.3, 129.2, 131.8, 132.6, 142.7, 159.2, 162.2, 168.1, 195.6. Anal. Calcd. for $C_{20}H_{23}ClN_2O_3$: C, 64.08; H, 6.18; N, 7.47. Found: C, 63.96; H, 5.98; N, 7.53.

Ethyl 2-amino-1,4,5,6,7,8-hexahydro-4-(4-methoxyphenyl)-7,7-dimethyl-5-oxoquinoline-3-carboxylate (5i): Light yellow solid, mp 128°C–130°C. [122°C–125°C Lit. (Kumar et al., 2008)]. IR (KBr) υ_{max} (cm^{-1}): 3413 (NH_2), 3304 (NH_2), 3226 (NH), 1690 (C=O), 1668 (C=O), 1621 (C=C), 1288 (C-O), 1036 (C-N). ^{1}H NMR (500 MHz, $CDCl_3$): δ (ppm) = 0.89 (s, 3H), 1.02 (s, 3H), 1.09 (t, 3H, J = 7.0 Hz), 2.04 (d, 1H, J = 20.0 Hz), 2.24 (d, 1H, J = 20.0 Hz), 2.46 (s, 2H), 3.66 (s, 3H), 3.90–3.97 (m, 2H), 4.44 (s, 1H), 6.75 (d, 2H, J = 5.0 Hz), 7.02 (d, 2H, J = 5.0 Hz), 7.49 (s, 2H, NH_2). ^{13}C NMR (125.72 MHz, $CDCl_3$): δ (ppm) = 14.7, 26.9, 29.1, 32.3, 32.8, 40.5, 50.5, 55.3, 59.2, 78.5, 113.5, 116.2, 129.0, 138.9, 157.7, 159.5, 162.5, 168.5, 196.2.

Ethyl 2-amino-4-(4-fluorophenyl)-1,4,5,6,7,8-hexahydro-7,7-dimethyl-5-oxoquinoline-3-carboxylate (5j): Light yellow solid, mp 155°C–158°C. IR (KBr) υ_{max} (cm^{-1}): 3402 (NH_2), 3289 (NH_2), 3212 (NH), 1693 (C=O), 1659 (C=O), 1611 (C=C), 1290 (C-O), 1039 (C-N). ^{1}H NMR (500 MHz, $CDCl_3$): δ (ppm) = 0.87 (s, 3H), 1.01 (s, 3H), 1.06 (t, 3H, J = 7.05 Hz), 2.05 (d, 1H, J = 16.05 Hz), 2.24 (d, 1H, J = 16.05 Hz), 2.49 (s, 2H), 3.93 (q, 2H, J = 7.05 Hz), 4.49 (s, 1H), 7.00 (t, 2H, J = 3.05 Hz), 7.13–7.16 (m, 2H), 7.57 (s, 2H, NH_2). ^{13}C NMR (125.72 MHz, $CDCl_3$): δ (ppm) = 14.6, 26.9, 29.0, 32.3, 33.1, 40.0, 50.39, 59.2, 78.1, 114.8, 115.8, 129.9, 143.0, 159.6, 160.9, 162.5, 168.3, 196.2.

Ethyl 2-amino-1,4,5,6,7,8-hexahydro-4-(3,5-dimethoxyphenyl)-7,7-dimethyl-5-oxoquinoline-3-carboxylate (5k): Light yellow solid, mp 222°C–226°C. IR (KBr) υ_{max} (cm^{-1}): 3436 (NH_2), 3304 (NH_2), 3197 (NH), 1690 (C=O), 1663 (C=O), 1592 (C=C), 1285 (C-O), 1038 (C-N). ^{1}H NMR (500 MHz, $CDCl_3$): δ (ppm) = 1.03 (s, 3H), 1.10 (s, 3H), 1.22 (t, 3H, J =7.2 Hz), 2.22 (d, 1H, J = 16.2 Hz), 2.26 (d, 1H, J = 16.2 Hz), 2.40 (s, 2H), 3.78 (s, 6H), 4.06–4.13 (m, 2H), 4.70 (s, 1H), 6.23 (s, 2H, NH_2) 6.27 (t, 1H, J = 1.6 Hz), 6.48 (d, 2H, J = 2.0 Hz). ^{13}C NMR (125.72 MHz, $CDCl_3$): δ (ppm) = 14.0, 26.9, 29.1, 32.0, 34.2, 41.0, 51.0, 55.3, 60.1, 80.1, 98.0, 117.0, 148.0, 158.1, 160.0, 161.0, 169.2, 196.0. Anal. Calcd. for $C_{22}H_{28}N_2O_5$: C, 65.98; H, 7.05; N, 7.00. Found: C, 65.88; H, 7.03; N, 7.20.

Acknowledgment: We are thankful to the Yazd University Research Council for partial support of this work.

References

Abdollahi-Alibeik, M.; Hoseinikhah, S. S. $ClO4^-$/Zr-MCM-41 nanoparticles prepared at mild conditions: a novel solid acid catalyst for the synthesis of polyhydroquinolines. *J. Iran Chem. Soc.* **2016**, *13*, 1339–1347.

Abdollahi-Alibeik, M.; Pouriayevali, M. 12-Tungstophosphoric acid supported on nano sized MCM-41 as an efficient and reusable solid acid catalyst for the three-component imino Diels–Alder reaction. *React. Kinet. Mech. Cat.* **2011**, *104*, 235–248.

Abdollahi-Alibeik, M.; Rezaeipoor-Anari, A. BF3/MCM-41 as nano structured solid acid catalyst for the synthesis of 3-iminoaryl-imidazo[1,2-a]pyridines. *Cat. Sci. Tech.* **2014**, *4*, 1151–1159.

Abdollahi-Alibeik, M.; Rezaeipoor-Anari, A. MCM-41 functionalized with B-F bond: preparation, characterization and catalytic application in the synthesis of polyhydroquinolines. *Lett. Org. Chem.* **2015**, *12*, 651–658.

Abdollahi-Alibeik, M.; Rezaeipoor-Anari, A. Fe3O4@B-MCM-41: a new magnetically recoverable nanostructured catalyst for the synthesis of polyhydroquinolines. *J. Magn. Magn. Mater.* **2016**, *398*, 205–214.

Adharvana Chari, M.; Syamasundar, K. Silica gel/$NaHSO_4$ catalyzed one-pot synthesis of Hantzsch 1,4-dihydropyridines at ambient temperature. *Catal. Commun.* **2005**, *6*, 624–626.

Araki, H.; Fukuoka, A.; Sakamoto, Y.; Inagaki, S.; Sugimoto, N.; Fukushima, Y.; Ichikawa, M. Template synthesis and characterization of gold nano-wires and particles in mesoporous channels of FSM-16. *J. Mol. Catal. A: Chem.* **2003**, *199*, 95–102.

Boer, R.; Gekeler, V. Chemosensitizers in tumor therapy: new compounds promise better efficacy. *Drug Future* **1995**, *20*, 499–510.

Bretzel, R.; Bollen, C.; Maeser, E.; Federlin, K. Trombodipine platelet aggregation inhibitor antithrombotic. *Drug Future* **1992**, *17*, 465.

Bretzel, R.; Bollen, C.; Maeser, E.; Federlin, K. Nephroprotective effects of nitrendipine in hypertensive type I and type II diabetic patients. *Am. J. Kidney Dis.* **1993**, *21*, 53.

Das, B.; Ravikanth, B.; Ramu, R.; Vittal Rao, B. An efficient one-pot synthesis of polyhydroquinolines at room temperature using HY-zeolite. *Chem. Pharm. Bull.* **2006**, *54*, 1044–1045.

Davis, H.; Davis, T. Daunorubicin and adriamycin in cancer treatment: an analysis of their roles and limitations. *Cancer Treat. Rep.* **1979**, *63*, 809–815.

Dondoni, A.; Massi, A.; Minghini, E.; Bertolasi, V. Multicomponent Hantzsch cyclocondensation as a route to highly functionalized 2-and 4-dihydropyridylalanines, 2- and 4-pyridylalanines, and their *N*-oxides: preparation via a polymer-assisted solution-phase approach. *Tetrahedron* **2004**, *60*, 2311–2326.

Donelson, J. L.; Gibbs, R. A.; De, S. K. An efficient one-pot synthesis of polyhydroquinoline derivatives through the Hantzsch four component condensation. *J. Mol. Catal. A: Chem.* **2006**, *256*, 309–311.

Guo, S.; Yuan, Y. One-pot synthesis of 1,4-dihydropyridine and polyhydro-quinoline derivatives via L-proline catalyzed Hantzsch multicomponent reaction under ultrasound irradiation. *Chin. J. Chem.* **2010**, *28*, 811–817.

Hantzsch, A. Ueber die synthese pyridinartiger verbindungen aus acetessigäther und aldehydammoniak. *Justus Liebigs Ann. Chem.* **1882**, *215*, 1–82.

Hong, M.; Cai, C.; Yi, W.-B. Hafnium (IV) bis(perfluorooctanesulfonyl) imide complex catalyzed synthesis of polyhydroquinoline derivatives via unsymmetrical Hantzsch reaction in fluorous medium. *J. Fluorine Chem.* **2010**, *131*, 111–114.

Inagaki, S.; Fukushima, Y.; Kuroda, K. Synthesis of highly ordered mesoporous materials from a layered polysilicate. *J. Chem. Soc., Chem. Commun.* **1993**, 680–682.

Inagaki, S.; Koiwai, A.; Suzuki, N.; Fukushima, Y.; Kuroda, K. Syntheses of highly ordered mesoporous materials, FSM-16, derived from kanemite. *Bull. Chem. Soc. Jpn.* **1996**, *69*, 1449–1457.

Karade, N. N.; Budhewar, V. H.; Shinde, S. V.; Jadhav, W.N. L-Proline as an efficient organo-catalyst for the synthesis of polyhydroquinoline via multicomponent Hantzsch reaction. *Lett. Org. Chem.* **2007**, *4*, 16–19.

Kassaee, M. Z.; Masrouri, H.; Movahedi, F. ZnO-nanoparticle-promoted synthesis of polyhydroquinoline derivatives via multicomponent Hantzsch reaction. *Monatsh. Chem.* **2010**, *141*, 317–322.

Khaligh, N. G. 1,1′-Butylenebis(3-methyl-3H-imidazol-1-ium) hydrogen sulfate catalyzed one-pot multi-component synthesis of unsymmetrical polyhydroquinoline derivatives. *Polycyclic Aromat. Compd.* **2016**, *36*, 284–294.

Klusa, V. Cerebrocrast. Neuroprotectant, cognition enhancer. *Drug Future* **1995**, *20*, 135–138.

Ko, S.; Yao, C.-F. Ceric ammonium nitrate (CAN) catalyzes the one-pot synthesis of polyhydroquinoline via the Hantzsch reaction. *Tetrahedron* **2006**, *62*, 7293–7299.

Kumar, A.; Maurya, R. A. Bakers' yeast catalyzed synthesis of polyhydroquinoline derivatives via an unsymmetrical Hantzsch reaction. *Tetrahedron Lett.* **2007**, *48*, 3887–3890.

Kumar, A.; Maurya, R. A. Efficient synthesis of Hantzsch esters and polyhydroquinoline derivatives in aqueous micelles. *Synlett* **2008**, *2008*, 883–885.

Kumar, A.; Singh, P.; Saxena, A.; De, A.; Chandra, R.; Mozumdar, S. Nano-sized copper as an efficient catalyst for one pot three component synthesis of thiazolidine-2,4-dione derivatives. *Catal. Commun.* **2008**, *10*, 17–22.

Maheswara, M.; Siddaiah, V.; Damu, G. L. V.; Rao, C. V. An efficient one-pot synthesis of polyhydroquinoline derivatives via Hantzsch condensation using a heterogeneous catalyst under solvent-free conditions. *Arkivoc* **2006**, *2*, 201–206.

Mason, R. P.; Mak, I. T.; Trumbore, M. W.; Mason, P. E. Antioxidant properties of calcium antagonists related to membrane biophysical interactions. *Am. J. Cardiol.* **1999**, *84*, 16–22.

Mekheimer, R. A.; Hameed, A. A.; Sadek, K. U. Solar thermochemical reactions: four-component synthesis of polyhydroquinoline derivatives induced by solar thermal energy. *Green Chem.* **2008**, *10*, 592–593.

Moghaddam, F. M.; Saeidian, H.; Mirjafary, Z.; Sadeghi, A. Rapid and efficient one-pot synthesis of 1,4-dihydropyridine and polyhydroquinoline derivatives through the Hantzsch four component condensation by zinc oxide. *J. Iranian Chem. Soc.* **2009**, *6*, 317–324.

Nagarapu, L.; Kumari, M. D.; Kumari, N. V.; Kantevari, S. MCM-41 catalyzed rapid and efficient one-pot synthesis of polyhydroquinolines via the Hantzsch reaction under solvent-free conditions. *Catal. Commun.* **2007**, *8*, 1871–1875.

Pastan, I.; Gottesman, M. Multiple-drug resistance in human cancer. *N. Engl. J. Med.* **1987**, *316*, 1388–1393.

Pasunooti, K. K.; Nixon Jensen, C.; Chai, H.; Leow, M. L.; Zhang, D.-W.; Liu, X.-W. Microwave-assisted copper (II)-catalyzed one-pot four-component synthesis of multifunctionalized dihydropyridines. *J. Comb. Chem.* **2010**, *12*, 577–581.

Pizzio, L. R.; Vázquez, P. G.; Cáceres, C. V.; Blanco, M. N. Supported Keggin type heteropolycompounds for ecofriendly reactions. *Appl. Catal. A Gen.* **2003**, *256*, 125–139.

Ranjbar-Karimi, R.; Hashemi-Uderji, S.; Bazmandegan-Shamili, A. MgO nanoparticles as a recyclable heterogeneous catalyst for the synthesis of polyhydroquinoline derivatives under solvent free conditions. *Chin. J. Chem.* **2011**, *29*, 1624–1628.

Reddy, C. S.; Raghu, M. Facile ZrCl4 promoted four-component coupling one-pot synthesis of polyhydroquinoline derivatives through unsymmetric Hantzsch reaction. *Indian J. Chem., Sect. B: Org. Chem. Incl. Med. Chem.* **2008**, *47*, 1578.

Saha, M.; Pal, A. K. Palladium(0) nanoparticles: an efficient catalyst for the one-pot synthesis of polyhydroquinolines. *Tetrahedron Lett.* **2011**, *52*, 4872–4877.

Saha, M.; Luireingam, T. S.; Merry, T.; Pal, A. K. Catalyst-free, Knoevenagel–Michael addition reaction of dimedone under microwave irradiation: an efficient one-pot synthesis of polyhydroquinoline derivatives. *J. Heterocycl. Chem.* **2013**, *50*, 941–944.

Song, G.; Wang, B.; Wu, X.; Kang, Y.; Yang, L. Montmorillonite K10 clay: an effective solid catalyst for one-pot synthesis of polyhydroquinoline derivatives. *Synth. Commun.* **2005**, *35*, 2875–2880.

Tu, S.; Zhang, J.; Zhu, X.; Zhang, Y.; Wang, Q.; Xu, J.; Shi, F. One-pot synthesis of hexahydroquinolines via a four-component cyclocondensation under microwave irradiation in solvent free conditions: a green chemistry strategy. *J. Heterocycl. Chem.* **2006**, *43*, 985–988.

Wang, L.-M.; Sheng, J.; Zhang, L.; Han, J.-W.; Fan, Z.-Y.; Tian, H.; Qian, C.-T. Facile Yb(OTf)3 promoted one-pot synthesis of polyhydroquinoline derivatives through Hantzsch reaction. *Tetrahedron* **2005**, *61*, 1539–1543.

Yanagisawa, T.; Shimizu, T.; Kuroda, K.; Kato, C. The preparation of alkyltrimethylammonium-kanemite complexes and their conversion to microporous materials. *Bull. Chem. Soc. Jpn* **1990**, *63*, 988–992.